Wavelet and multiwavelet watermarking

C.V. Serdean, M.K. Ibrahim, A. Moemeni and M.M. Al-Akaidi

Abstract: The main objective of the paper is to provide a like-with-like performance comparison between the wavelet domain and the multiwavelet domain watermarking, under a variety of attacks. The investigation is restricted to balanced multiwavelets. Furthermore, for multiwavelet domain watermarking, both wavelet-style and multiwavelet-style embedding are investigated. It was shown that none of the investigated techniques performs best across the board. The wavelet-style multiwavelet technique is best suited for compression attacks, whereas scalar wavelets are superior under cropping and scaling. The multiwavelet-style multiwavelet is far superior under low-pass filtering. On the basis of these results, it was concluded that for attacks which are likely to affect mid-range frequencies, the wavelets are more suitable than multiwavelets, whereas for attacks which are likely to affect low frequencies or high frequencies, the multiwavelets are the best choice. Furthermore, the multiwavelets generally offer better visual quality than scalar wavelets, for the same peak signal-to-noise ratio (PSNR). This suggests that part of the available channel capacity remains unused, and shows once more the potential of multiwavelets for digital watermarking.

1 Introduction

Recent research in fields such as watermarking and compression has shown the many advantages of the wavelet transform over traditional block-based discrete cosine transform (DCT) methods. In order to offer the best performance in a range of image-processing applications – including watermarking and compression – the wavelet transform requires filters that combine a number of desirable properties, such as compact support, orthogonality, symmetry, filter regularity and smoothness. However, the design possibilities for wavelets are limited; notably the wavelets cannot simultaneously achieve orthogonality and symmetry. The discrete multiwavelet transform (DMWT) has been specifically designed to address this problem [1, 2]. By employing multiple filters, the DMWT provides more degrees of freedom than a traditional scalar wavelet and therefore can offer orthogonality, symmetry and high order of approximation simultaneously.

Although there are plenty of papers addressing the use of wavelet transforms in watermarking, there are only a handful of papers addressing the relatively new multiwavelet transform in watermarking applications [3–8]. Some of the early investigations into multiwavelet-based watermarking techniques report moderate or no robustness improvements over scalar wavelets, or in some cases even over the classical DCT methods [3]. Other papers limit their investigation to a narrower application area, such as the non-blind system described in [4] or the techniques proposed in [5, 6] which fuse an invisible logo in the host image. Most of these systems are based on the classical spread-spectrum approach employed by Cox *et al.* [9]. The majority of these papers describe '1-bit' systems, as watermark recovery yields a simple yes/no answer with respect to the presence of the watermark or visual logo. Issues such as high-capacity watermarking, visual-model-based embedding and channel capacity are just starting to appear [7].

The techniques employed by various authors to obtain a robust, adaptive watermark range from using existing perceptual models adapted to the DMWT [8] to employing neural networks or genetic algorithms [5, 8] In general, a common feature of these media adaptive techniques is their complexity.

The technique proposed here aims for a much simpler perceptual model (as described in Section 3.1), which embeds an adaptive (both perceptually dependent and media-dependent), hierarchical (Section 3.3), high-capacity watermark. Unlike most other papers, this work is directed towards balanced multiwavelets and investigates systematically the impact of both wavelet-style and multiwavelet-style decomposition of the DMWT coefficients. The main objective is to provide a like-with-like performance comparison between the wavelet and the multiwavelet watermarking, under a variety of attacks. These results are used to analyse the strengths and weaknesses of both wavelets and multiwavelets (for both wavelet- and multiwavelet-style embedding). The proposed techniques benefit from state-of-the-art error correction and hierarchical watermark embedding/retrieval. The performance of the three techniques is evaluated in terms of channel capacity under various attacks.

2 Multiwavelet transform

Any good transform should possess several important properties: orthogonality, to ensure the decorrelation of sub-band coefficients; symmetry (i.e. linear phase) to process finite-length signals without redundancy and artefacts and finite-length filters for computational efficiency. However, most real scalar wavelet transforms fail to possess these properties simultaneously. To circumvent these limitations, multiwavelets have been proposed

© The Institution of Engineering and Technology 2007

doi:10.1049/iet-ipr:20060214

Paper first received 6th April and in revised form 8th December 2006

The authors are with the School of Engineering and Technology, De Montfort University, The Gateway, Leicester LE1 9BH, UK

E-mail: cvs@dmu.ac.uk

where orthogonality and symmetry are allowed to co-exist by relaxing the time-invariant constraint [10].

Multiwavelets may be considered as a generalisation of scalar wavelets. However, some important differences exist between these two types of multiresolution transforms. In particular, scalar wavelets have a single scaling $\phi(t)$ and wavelet function $\psi(t)$, whereas multiwavelets may have two or more scaling and wavelet functions. In general, a multiwavelet transform can have r scaling functions and r corresponding wavelet functions. To date, most existing multiwavelets have $r = 2$. For this particular case, one can write the scaling and, respectively, wavelet functions using the vector notation

$$\begin{aligned} \boldsymbol{\Phi}(t) &= [\phi_1(t) \quad \phi_2(t)]^{\mathrm{T}} \\ \boldsymbol{\Psi}(t) &= [\psi_1(t) \quad \psi_2(t)]^{\mathrm{T}} \end{aligned} \tag{1}$$

where $\boldsymbol{\Phi}(t)$ is called the multiscaling function and $\boldsymbol{\Psi}(t)$ the multiwavelet function. The $r = 1$ case corresponds to a scalar wavelet (discrete wavelet transform). As for scalar wavelets, the following equations have to be satisfied

$$\begin{aligned} \boldsymbol{\Phi}(t) &= \sqrt{2} \sum_{k=-\infty}^{+\infty} \boldsymbol{H}_k \boldsymbol{\Phi}(2t-k) \\ \boldsymbol{\Psi}(t) &= \sqrt{2} \sum_{k=-\infty}^{+\infty} \boldsymbol{G}_k \boldsymbol{\Psi}(2t-k) \end{aligned} \tag{2}$$

For multiwavelets, both $\{\boldsymbol{H}_k\}$ and $\{\boldsymbol{G}_k\}$ are 2×2 matrices of filters

$$\begin{aligned} \boldsymbol{H}_k &= \begin{bmatrix} h_0(2k) & h_0(2k+1) \\ h_1(2k) & h_1(2k+1) \end{bmatrix} \\ \boldsymbol{G}_k &= \begin{bmatrix} g_0(2k) & g_0(2k+1) \\ g_1(2k) & g_1(2k+1) \end{bmatrix} \end{aligned} \tag{3}$$

where $\{h_k(n)\}$ and $\{g_k(n)\}$ are, respectively, the scaling and wavelet filter sequences such that $\sum_n h_k^2(n) = 1$ and $\sum_n g_k^2(n) = 1$, for $k = 1, 2$.

This matrix of filters provides more degrees of freedom than a traditional scalar wavelet. Because of these extra degrees of freedom, multiwavelets can achieve simultaneously orthogonality, symmetry and high order of approximation (vanishing moments).

2.1 Multiwavelet filter bank

Similar to the scalar wavelet case, one can describe the multiwavelet transform using a filter bank representation. For multiwavelets, this translates into a multi-input multi-output filter bank, as illustrated in Fig. 1. In case of a one-dimensional (1D) signal, it requires vectorisation of the input signal to produce an input signal that is r-dimensional. This can be achieved by splitting the 1D signal into its polyphase components. Therefore, the matrix filter bank, given in (3), can be transformed into a simple time-varying multichannel filter bank described by

$$\begin{aligned} \begin{bmatrix} H_0(z) \\ H_1(z) \end{bmatrix} &= H(z^2) \begin{bmatrix} 1 \\ z^{-1} \end{bmatrix} \\ \begin{bmatrix} G_0(z) \\ G_1(z) \end{bmatrix} &= G(z^2) \begin{bmatrix} 1 \\ z^{-1} \end{bmatrix} \end{aligned} \tag{4}$$

where $H_0(z)$ and $H_1(z)$ are the z transforms of the two low-pass branch filters h_0 and h_1. Similarly, $G_0(z)$ and $G_1(z)$ are the transforms of the two high-pass branch filters g_0 and g_1. The resulting time-varying multiwavelet filter bank structure is illustrated in Fig. 2. The separability property of the multiwavelet transform can be exploited in order to build a 2D multiwavelet transform.

2.2 Balanced against unbalanced multiwavelets

Lebrun and Vetterli [10] showed that if the associated scalar polyphase filters within a branch have different spectral behaviour, for example, low-pass behaviour for one case and high pass for another, then this leads to unbalanced channels that complicate the vectorisation process. The vectorisation process would lead to channels that mix the approximation and detail coefficients creating strong oscillations in the signal reconstructed from the low-pass sub-band coefficients only.

The unbalanced multiwavelets need to compensate for this by employing pre/post-filtering of the input/output signal to adapt it to the spectral imbalance of the filter bank.

The balanced multiwavelets impose by design that a certain class of polynomial signals has to be preserved by the low-pass branch and cancelled by the high-pass branch. For example, a multiwavelet is said to be balanced of order 1, if the low-pass synthesis preserves constant signals. A multiwavelet is said to be balanced of order p if the low-pass synthesis preserves discrete-time polynomial signals of degree less than p. Balancing obviates the need for input pre-filtering; thus, balanced multiwavelets are computationally more efficient than the unbalanced multiwavelets.

2.3 Multiwavelet decomposition and sub-band re-shuffling

The multichannel nature of multiwavelets yields a different sub-band structure compared with scalar wavelets. In the 2D transform case, the DMWT analyses the input in 16 sub-bands instead of the usual four sub-bands of scalar wavelet transforms. This can be observed in Fig. 3 for two levels of decomposition. The multiwavelet decomposition structure of the BAT02 [11] multiwavelet is shown in Fig. 3*b* in contrast with the wavelet decomposition of the Antonini 9.7 scalar wavelet in Fig. 3*a*. The different multiwavelet decomposition structure creates 'incompatibility' problems

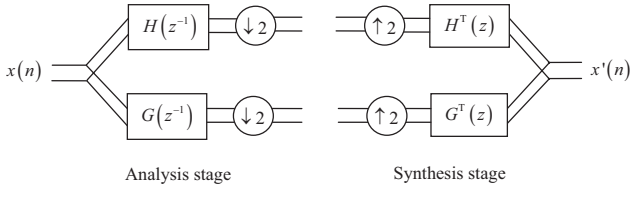

Fig. 1 *Perfect reconstruction orthogonal multiwavelet filter bank for r = 2*

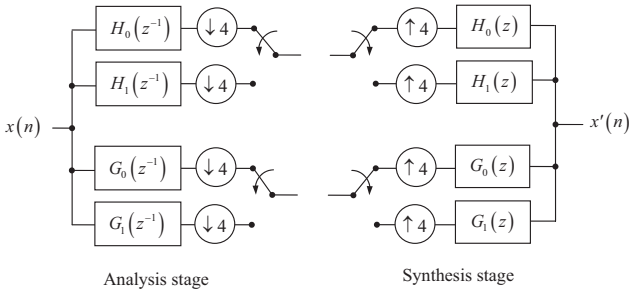

Fig. 2 *Time-varying multiwavelet filter bank for r = 2*

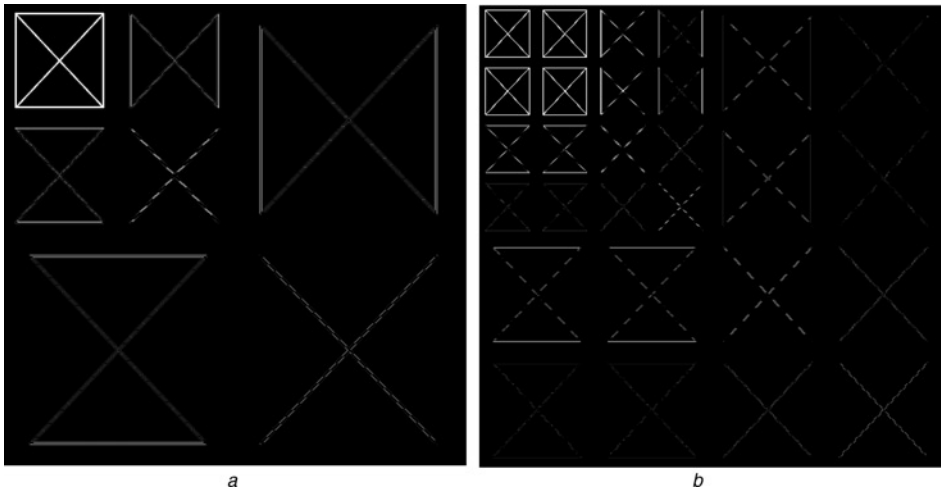

Fig. 3 *Two levels of decomposition*
a Antonini 9.7 scalar wavelet
b BAT02 multiwavelet

for a range of applications, particularly in compression [12]. One cannot simply directly replace a scalar wavelet with a multiwavelet and reap the benefits offered by the multiwavelets.

However, one can use the shuffling technique proposed by Martin and Bell [12], to rearrange the multiwavelet coefficients in order to obtain a decomposition structure similar to that of the scalar wavelets. Although this technique works very well for balanced wavelets, it is not suitable for unbalanced multiwavelets as the resulting sub-bands are not a faithful spatio-frequency representation of the input image.

3 Proposed multiwavelet watermarking system

The proposed multiwavelet-based watermarking system is presented in Fig. 4. Watermark embedding uses the established blind spread-spectrum approach and as such retrieval is via cross-correlation. The main features of the proposed system are: (a) embeds a perceptual, image-adaptive watermark in all multiwavelet coefficients, (b) embeds a self-contained watermark in each sub-band independently, enabling hierarchical watermark embedding/recovery and (c) maximises the capacity of the watermarking channel by employing powerful state-of-the-art error correction.

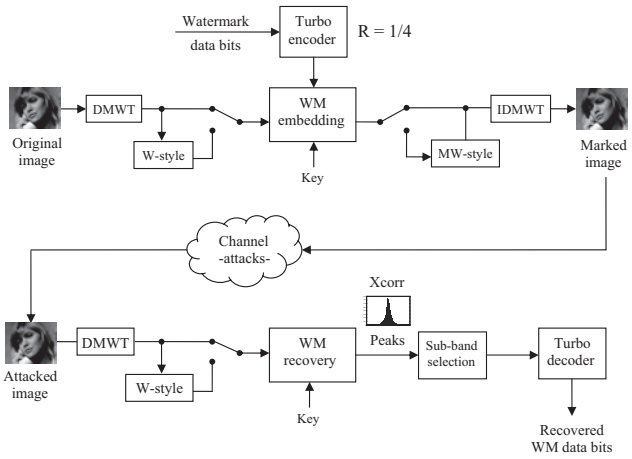

Fig. 4 *Multiwavelet watermarking system*

3.1 Perceptual, image-adaptive watermarking of multiwavelet coefficients

As one of the objectives is to investigate the advantages and the disadvantages of multiwavelet watermarking with and without coefficient reshuffling [12], the same embedding formula will be used in both cases. This will facilitate the direct comparison between the two schemes. The watermark is embedded using amplitude modulation, that is, $C^{\mathrm{M}}_{i,j} = C_{i,j} + S \cdot W_{i,j}$, with the embedding strength S defined as

$$S = \alpha \cdot w(\lambda) \cdot \frac{\boldsymbol{Q}(\lambda, \theta)}{Q_{\min}} \cdot \frac{|C_{i,j}|}{\mathrm{mean}(C_{i,j})} \tag{5}$$

where $Q_{\min}$ is the minimum value from matrix $\boldsymbol{Q}$, $W_{i,j}$ the watermark, $C_{i,j}$ the original wavelet coefficient, $C^{\mathrm{M}}_{i,j}$ the marked coefficient and $w(\lambda)$ a level-dependent weighting factor.

Note that (5) incorporates both perceptual and media dependence which is essential for robust watermarking. This marks more heavily the high-frequency sub-bands (as $\boldsymbol{Q}(\lambda, \theta)/Q_{\min}$ returns a higher value) and the largest coefficients (as $|C_{i,j}|/\mathrm{mean}(C_{i,j})$ increases), because modification of these coefficients is less likely to incur visible artefacts (media dependence).

The perceptual component is incorporated in the quantisation matrix $\boldsymbol{Q}(\lambda, \theta)$, where λ is the level and θ denotes the orientation. For computing $\boldsymbol{Q}(\lambda, \theta)$, the perceptual model developed by Watson *et al.* [13] for the Antonini 9.7 scalar wavelet is used. As currently there are no established human visual system models available for the multiwavelets, the same quantisation matrix will also be used for multiwavelets. Although this might not be an optimal solution, the fact that the proposed embedding method does not directly use the actual values of the quantisation factors, but their relative weight $(\boldsymbol{Q}(\lambda,\theta)/Q_{\min})$ partly compensates for this drawback. The use of the sub-band weighting factor $w(\lambda)$ allows us to further compensate for this. Experimental results show that in spite of the un-optimised quantisation matrix, the proposed multiwavelet system still delivers good perceptual transparency (PSNR = 37–38 dB) and watermark robustness. Once a more suitable perceptual model is developed, this can be exploited to further optimise the embedding process. For the multiwavelet-style system, the four resulting sub-bands

corresponding to one wavelet-style sub-band (Fig. 3) use the same relative weighting factor, but adapt themselves to the local coefficient strength and the average coefficient value of each of the four sub-bands.

3.2 Maximising watermarking channel capacity through error correction

Most novel high-capacity watermarking systems use various forms of error correction to increase the robustness of the system under attack and to increase the information capacity of the channel. In the proposed system, the watermark is protected by employing a rate 1/4 multiple parallel-concatenated convolutional code (MPCCC), because of its superior performance over classical parallel-concatenated convolutional codes (PCCCs). Previous work carried out under both the DCT and wavelet framework shows that such a code can significantly increase the capacity and the robustness of the watermark [14, 15]. The details of the specific code used in this work can be found in [14].

3.3 Self-contained watermark embedding and automated recovery

Different types of attacks are likely to affect the different multiwavelet sub-bands differently, depending on the nature of the attack and the frequency content of each sub-band. Indeed, this behaviour can be observed in Section 5. In recognition of this aspect, an independent, self-contained spread-spectrum watermark (all data bits) has been embedded in each multiwavelet sub-band [16]. Correlation is therefore performed separately for each sub-band, obtaining a set of cross-correlation peaks (one peak for each embedded data bit) for each multiwavelet sub-band.

During the recovery process, the system calculates the signal-to-noise ratio (SNR) of the cross-correlation peaks for each sub-band, as well as the corresponding SNRs for various sub-band combinations. This information is used by the watermark-recovery system to automatically determine the optimal sub-band – or combination of sub-bands (based on the highest SNR) – for optimum watermark extraction. The coded watermark data bits are then recovered from the selected sub-band and sent to the turbo code decoder (Fig. 4).

The performance of the cross-correlator can be further improved by filtering the input image using a Laplacian 3×3 filter prior to cross-correlation [15, 16].

4 Comparative results under attack

By design, any watermarking system provides a trade-off among invisibility, robustness and capacity. All three aspects are addressed here: (a) the invisibility is assessed via objective visibility measurements (PSNR), (b) the robustness of the system is assessed against several types of attacks and (c) for each of these attacks, the capacity of the system is determined, as the maximum number of data bits which can be reliably extracted from the watermarked image for that particular type of attack. A watermark is considered to be reliably extracted if the bit error rate (BER) is 10^{-8} or lower. The intercept of the graphs presented in Figs. 5–10 with the x-axis (number of bits) represents the maximum number of bits (i.e. the capacity of the system) which can be reliably recovered for that specific type/strength of the attack.

The three systems have been tested with a number of attacks designed to illustrate the robustness of the watermark depending on the frequency ranges affected by these attacks. It should be noted that the magnitude of most of these attacks can be large enough to lead to serious-to-severe visibility artefacts, which in some cases would render the attacked image worthless. Increasing the magnitude of the attack to this extent is necessary in order to find the breaking point of the system and determine the capacity of the system. In spite of this, the watermark can still be recovered, showing the true extent of the robustness of the proposed system(s).

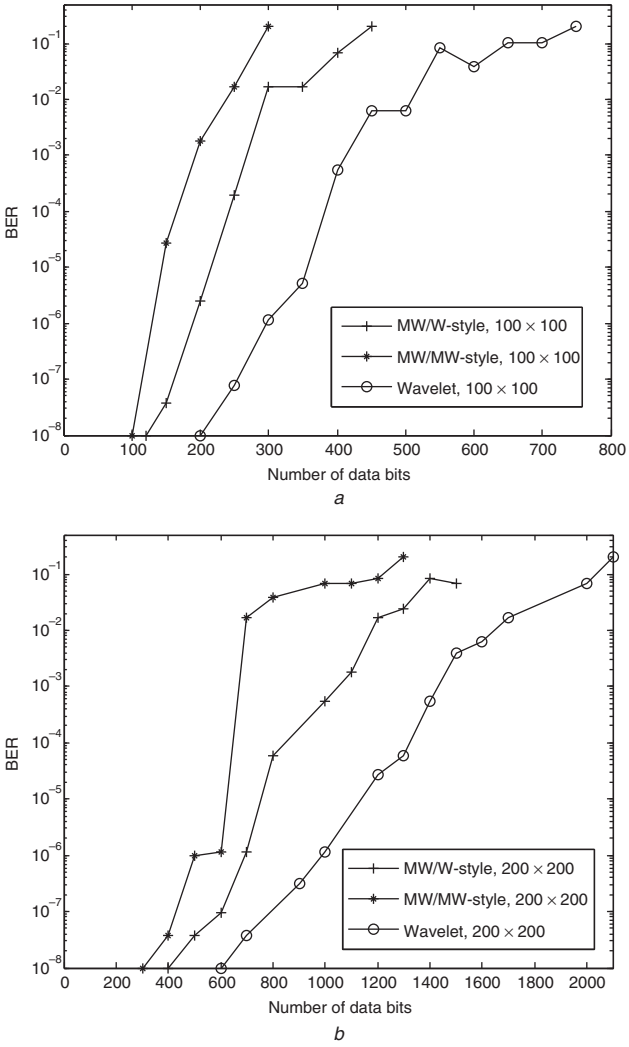

Fig. 5 *Performance of the system under cropping attack*
Cropped image sizes are
a 100 × 100
b 200 × 200

The multiwavelet selected for this work is BAT02. It is determined after carrying out a number of visibility tests that for the watermarking scheme employed here, this multiwavelet gave the lowest visibility artefacts out of the seven families of balanced multiwavelet tried. This is a 2-balanced multiwavelet designed by Lebrun and Vetterli [11]. All our experiments used three levels of decomposition, with the weighting factor $w(\lambda)$ being 2 for $\lambda = 3$ and 1 elsewhere. The global scaling factor α is set to 0.5.

The scalar wavelet watermarking system used here for comparison is presented in [16]. This system shares the same error-correcting features as the multiwavelet system described here. The embedding parameters have been scaled accordingly to match the PSNR given by the multiwavelet schemes.

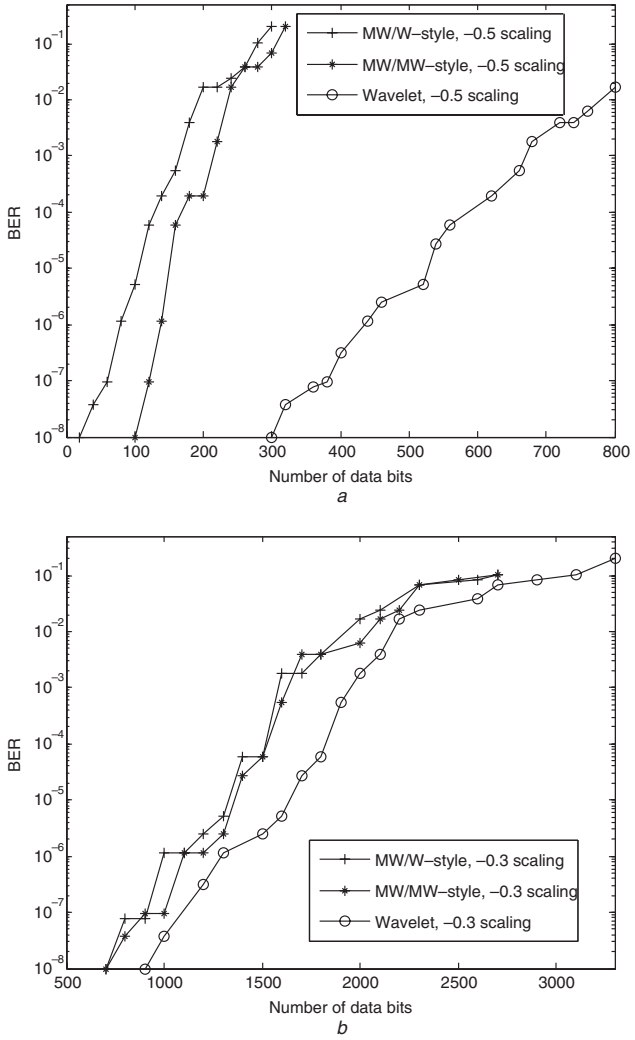

Fig. 6 *Performance of the system under scaling-rescaling attack*
Image is scaled down with a factor of
a 0.5
b 0.7

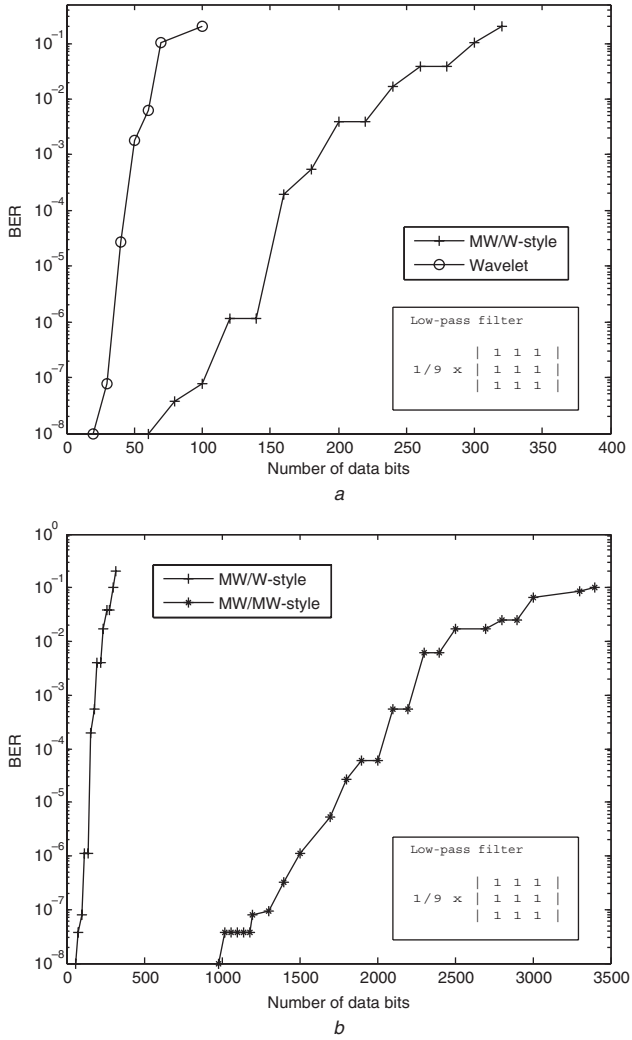

Fig. 7 *Performance of the system under aggressive low-pass filtering*
a Scalar wavelets against multiwavelets wavele-style
b Comparison between the two multiwavelet decomposition styles

In spite of similar PSNR values (37–38 dB), both multiwavelet systems consistently offer higher visual quality than the wavelet system. Similar visual quality results have been reported for compression by Martin and Bell [12].

The remainder of this section presents the comparative performance of the three systems under attack from the perspective of robustness against capacity for a given PSNR of 37–38 dB.

Fig. 5 illustrates the effects of cropping a small 100×100 and, respectively, 200×200 pixel area of an image. Cropping will affect lower frequencies more than the higher frequencies, because of the fact that the watermark in the higher levels corresponds to a smaller spatial support. At the same time, as just a small part of the watermarked image is available for cross-correlation, the SNR of the cross-correlation peaks worsens. Even for severe cropping, the channel capacity is in excess of 80 bits for both multiwavelet systems, with the scalar wavelets nearly doubling the channel capacity on average.

Scaling and rescaling back with the same factor, particularly when reducing the image size and intentionally using different interpolation filters during this process to increase the strength of the attack, will affect more the high frequencies than the low frequencies. Fig. 6*a* shows that when the image is scaled down to half of its original size and then rescaled back using nearest-neighbour interpolation, the scalar wavelets can triple channel capacity in comparison to the multiwavelets. For less stronger attacks, when the watermarked image is scaled down to 70% of its original size, this lead is still maintained (Fig. 6*b*), but it gets less obvious. Using bilinear interpolation instead of the nearest-neighbour interpolation currently used in the rescaling process reduces significantly the strength of this attack.

The effects of aggressive low-pass filtering, using an averaging 3×3 filter, are illustrated in Fig. 7. If the differences between scalar wavelets and wavelet-style multiwavelets favour the multiwavelets with a factor of 2 (Fig. 7*a*), the multiwavelet-style multiwavelet system achieves a remarkable lead (more than a 10-fold increase) over its sister wavelet-style multiwavelet. Coupled with the previous results, this suggests that multiwavelet-style embedding is superior to wavelet-style embedding for attacks, such as cropping, scaling and low-pass filtering.

This situation is completely reversed when it comes to compression (Fig. 8). Now the wavelet-style multiwavelets take the lead. Particularly under strong JPEG compression, the wavelet-style multiwavelets show nearly a 10-fold capacity increase over scalar wavelets, with the difference reducing to a factor of 3 for less aggressive compression.

This trend is also maintained for strong JPEG2000 compression, although for less aggressive compression, the scalar wavelets take again the lead. The reason for

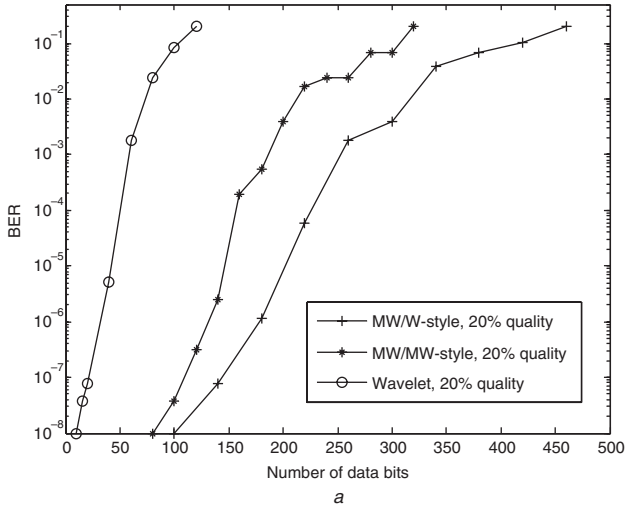

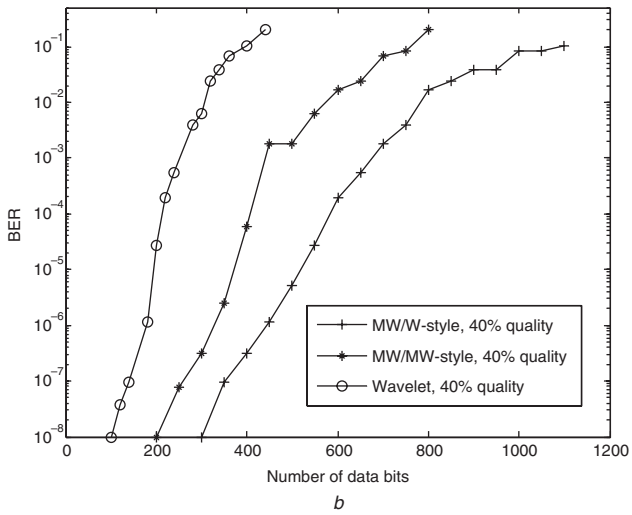

Fig. 8 *Performance of the system under low-quality JPEG compression*

a 20% quality
b 40% quality

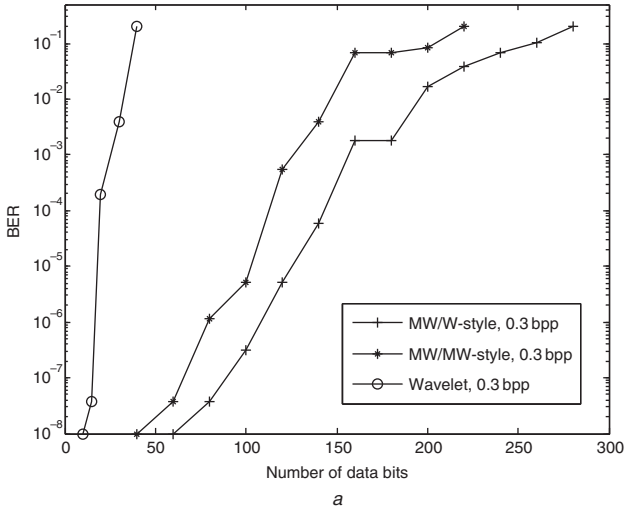

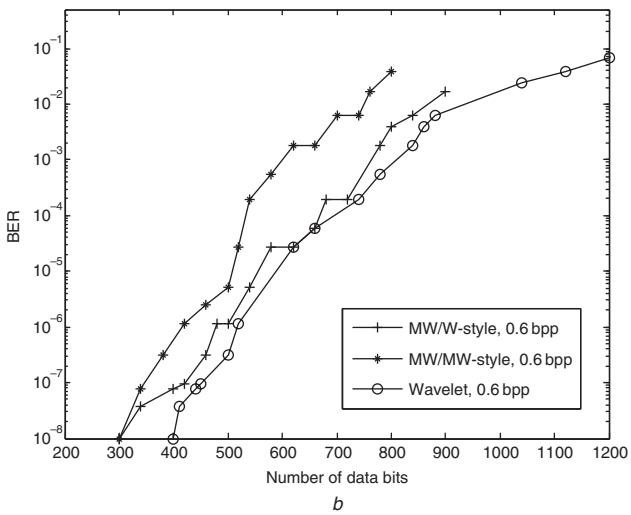

Fig. 9 *Performance of the system under low-quality JPEG2000 compression (JasPer)*

a 0.3 bpp
b 0.6 bpp

this is 2-fold. On one hand, this is because of the fact that the same wavelet used for compression is used for watermarking, and as such it is easier to compensate for the effects of the JPEG2000 compression. More importantly, when the watermark is embedded into the multiwavelet domain, and attacked in the scalar wavelet domain, the different sub-band frequency split of the multiwavelet and scalar wavelet filters tends to redistribute the watermark energy more evenly into the neighbouring sub-bands, and as such the JPEG2000 quantiser has an easier task in removing/weakening a larger percentage of the watermark.

Among the multiwavelet schemes, Figs. 7 and 8 show that the wavelet-style embedding is more suitable for compression than the multiwavelet-style embedding, suggesting that the first embeds a stronger high-frequency watermark, more robust to compression.

The impact of type I and type II collusion attacks on the three watermarking systems have also been studied. Type I collusion consists in averaging together several copies of the same image, with all copies containing different watermarks. Fig. 10*a* shows that the wavelet system significantly outperforms both multiwavelet systems. When the image marked with the original watermark is colluded with one extra copy carrying a different watermark, the wavelet system can accommodate 2.55 times more data bits than the multiwavelet counterparts, offering a capacity of 3700 bits (Fig. 10*a*). Notably, the two multiwavelet systems behave very much alike for this type of attack.

Type II collusion consists of embedding several different watermarks in the same host image, showing the behaviour of a watermarking system under a multiple watermarking scenario. The results are presented in Fig. 10*b*. For one or two extra watermarks, the wavelet system offers significantly better performance than both multiwavelet systems. Embedding three or four extra watermarks constitutes the cross-over point for the wavelet system with respect to its multiwavelet counterparts; when embedding four or more extra watermarks, both multiwavelet systems start to outperform the wavelet system. The wavelet-style multiwavelet system performs better than its multiwavelet-style counterpart, especially for less stronger attacks.

We have also benchmarked the three systems against high-pass filtering, edge-preserving low-pass filtering, and high-boost filtering, but these attacks do not constitute a significant threat for any of the three systems, and as such the results were not included.

The three systems presented here have not been designed to be natively robust against geometrical attacks, such as rotation and scaling; hence, in order to cope with these attacks, one would be required to conduct a very time-consuming extensive search. This is not the objective of this work. However, one can employ the 'plug-in' solution

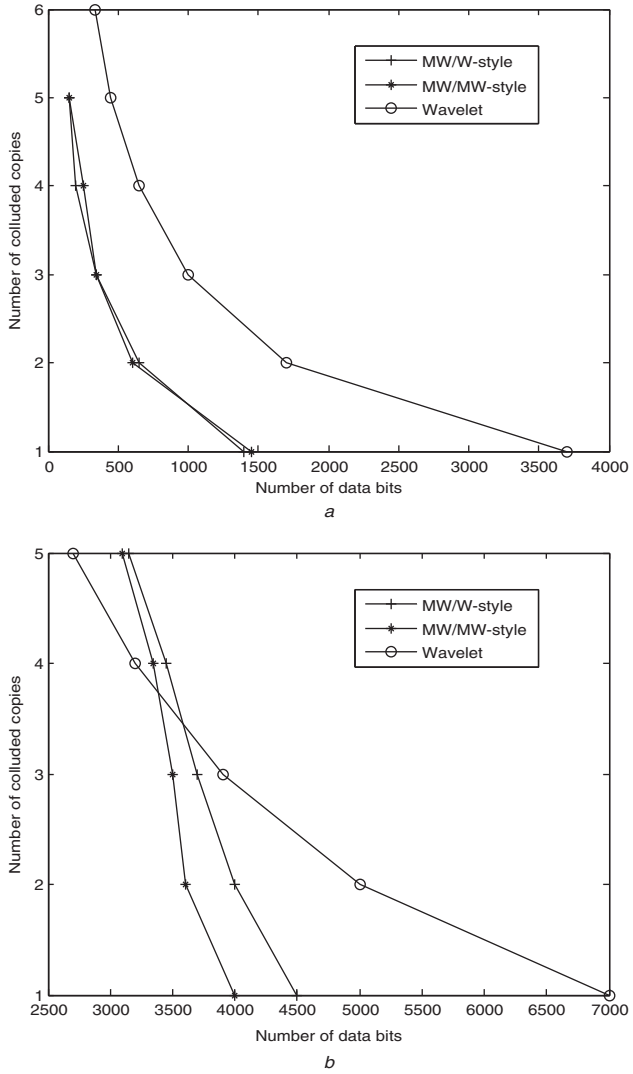

Fig. 10 *Performance of the system*
a Under type I collusion attack
b Under type II collusion attack

proposed by Serdean *et al.* [16], which uses a 1-bit reference spatial-domain watermark to undo the geometrical attack first, and then uses any of the systems proposed in this work to recover the main, high-capacity watermark. From the perspective of the main, high-capacity watermark, this 'undo' operation equates with a typical interpolation attack, as presented in Fig. 6 for scaling – rescaling (with similar results for rotation), and does not constitute a very strong attack, particularly when using bilinear interpolation in the rescaling process.

5 Conclusions

This research presented a like-with-like performance comparison among three techniques: wavelet domain watermarking, multiwavelet domain watermarking with a wavelet-style decomposition structure and multiwavelet domain watermarking with a multiwavelet-style decomposition structure.

Section 2 has shown that as a generalisation of scalar wavelets, the multiwavelets offer greater flexibility, and can possess simultaneously a number of desirable properties, and as such have the potential to improve a range of applications, watermarking included. The proposed multiwavelet watermarking techniques have been presented in Section 3, with the performance of these three techniques being discussed in Section 4. These results are summarised in Table 1.

Table 1: A summary of the performance under attack for the three systems

	Wavelet	Multiwavelet wavelet-style	Multiwavelet multiwavelet-style
Low-pass filtering	worst	average	best
Cropping	best	average	worst
Scaling	best	worst	average
JPEG	worst	best	average
JPEG2000 (low quality)	worst	best	average
JPEG2000 (high quality)	best	average	worst
Type I collusion	best	worst	worst
Type II collusion	best[a] worst[b]	average[a] best[b]	worst[a] average[b]

[a]For one to three colluded copies
[b]For ≥ 4 colluded copies

Furthermore, the difference between these techniques can also be summarised in terms of the highest SNR sub-band used for watermark recovery by each system. This alternative view is offered in Table 2, with the appropriate legend being presented in Fig. 11.

From the results presented in Tables 1 and 2, several conclusions are drawn. None of the presented techniques works best for all attacks. The wavelet-style multiwavelet technique is best suited for compression attacks, whereas scalar wavelets are superior under cropping and scaling. The multiwavelet-style multiwavelet is far superior under low-pass filtering. Combining this behaviour with the one presented in Table 2, one can conclude that for attacks which are likely to affect mid-range frequencies, the wavelets are more suitable than multiwavelets, whereas for attacks which are likely to affect low frequencies or high frequencies, the multiwavelets are the best choice.

Table 2: The highest SNR sub-bands selected by each system for watermark recovery, as a function of the attack

	Wavelet	Multiwavelet wavelet-style	Multiwavelet multiwavelet-style
Low-pass filtering	10	$4+7+10$	40
Cropping	10	10	$32+38+40$, $\text{sum}(n) \mid n = 29 \cdots 40$
Scaling	10	10, ALL, $8+9+10$	35, $32+38+40$
JPEG	10	ALL	$\text{sum}(n) \mid n = 29 \cdots 40$
JPEG2000	10	ALL	$\text{sum}(n) \mid n = 29 \cdots 40$
Type I and II collusion	10	ALL	$\text{sum}(n) \mid n = 29 \cdots 40$

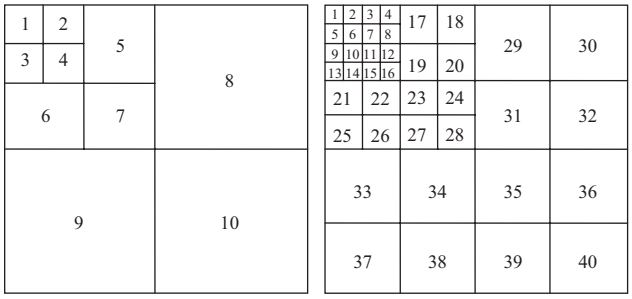

Fig. 11 *Scalar wavelet/wavelet-style multiwavelet*

a Against multiwavelet-style multiwavelet
b Sub-bands

In terms of visual artefacts, for the same PSNR, the multiwavelets tend to offer lower visual artefacts than scalar wavelets. This would suggest that part of the available channel capacity remains unused, and once suitable human visual models are developed for multiwavelets, the channel capacity and the robustness of these systems are likely to increase and even take the lead from scalar wavelets for attacks such as cropping and scaling.

6 References

1 Strela, V., Heller, P.N., Strang, G., Topiwala, P., and Heil, C.: 'The application of multiwavelet filterbanks to image processing', *IEEE Trans. Image Process.*, 1999, **8**, (4), pp. 548–563

2 Keinert, F.: 'Wavelets and multiwavelets' (Chapman and Hall/CRC, 2004), ISBN: 1-58488-304-9

3 Kumsawat, P., Attakitmongcol, K., and Srikaew, A.: 'The effects of transformation methods in image watermarking'. TENCON 2004, IEEE Region 10 Conf., 21–24 November 2004, vol. A, pp. 295–298

4 Zhao, J., Liu, Z., and Laganiere, R.: 'Digital watermarking by using a feature-based multiwavelet fusion approach'. Canadian Conf. on Electrical and Computer Engineering, 2–5 May 2004, vol. 1, pp. 563–566

5 Zhang, J., Wang, N.-C., and Xiong, F.: 'A novel watermarking for images using neural networks'. Proc. Int. Conf. on Machine Learning and Cybernetics, 4–5 November 2002, vol. 3, pp. 1405–1408

6 Kurugollu, F., Bouridane, A., Roula, M., and Boussakta, S.: 'Comparison of different wavelet transforms for fusion based watermarking applications'. Proc.10th IEEE Int. Conf. on Electronics, Circuits and Systems, ICECS 2003, 14–17 December 2003, vol. 3, pp. 1188–1191

7 Ghouti, L., Bouridane, A., Ibrahim, M.K., and Boussakta, S.: 'Digital image watermarking using balanced multiwavelets', *IEEE Trans. Signal Process.*, 2006, **54**, (4), pp. 1519–1536

8 Kumsawat, P., Attakitmongcol, K., and Srikaew, A.: 'A new approach for optimization in image watermarking by using genetic algorithms', *IEEE Trans. Signal Process.*, 2005, **53**, (12), pp. 4707–4719

9 Cox, I.J., Kilian, J., Leighton, T., and Shamoon, T.: 'Secure spread spectrum communication for multimedia', Technical Report 95-10, NEC Research Institute, 1995

10 Lebrun, J., and Vetterli, M.: 'Balanced multiwavelets: theory and design', *IEEE Trans. Signal Process.*, 1998, **46**, (4), pp. 1119–1125

11 Lebrun, J., and Vetterli, M.: 'High-order balanced multiwavelets: theory, factorisation and design', *IEEE Trans. Signal Process.*, 2001, **49**, (9), pp. 1918–1930

12 Martin, M.B., and Bell, A.E.: 'New image compression techniques multiwavelets and multiwavelet packets', *IEEE Trans. Image Process.*, 2001, **10**, (4), pp. 500–510

13 Watson, A.B., Yang, G., Solomon, J., and Villasenor, J.: 'Visibility of wavelet quantization noise', *IEEE Trans. Image Process.*, 1997, **6**, (8), pp. 1164–1175

14 Ambroze, M.A., Wade, J.G., Serdean, C.V., Tomlinson, M., Stander, J., and Borda, M.: 'Turbo code protection of a video watermarking channel', *IEE Proc., Vis. Image Signal Process.*, 2001, **148**, (1), pp. 54–58

15 Serdean, C.V.: 'Spread spectrum-based video watermarking algorithms for copyright protection', Ph.D. thesis, University of Plymouth, UK, August 2002 (URL:http://www.serdean.com/downloads.htm)

16 Serdean, C.V., Ambroze, M.A., Tomlinson, M., and Wade, J.G.: 'DWT based high capacity blind video watermarking, invariant to geometrical attacks', *IEE Proc., Vis. Image Signal Process.*, 2003, **150**, (1), pp. 51–58